JOURNAL OF VIROLOGY, Apr. 2002, p. 3659–3669 Vol. 76, No. 8
0022-538X/02/$04.00+0 DOI: 10.1128/JVI.76.8.3659–3669.2002

Recognition of the Measles Virus Nucleocapsid as a Mechanism of IRF-3 Activation

Benjamin R. tenOever,[1,2] Marc J. Servant,[1,2] Nathalie Grandvaux,[1,2] Rongtuan Lin,[1,2] and John Hiscott[1,2,3]*

Terry Fox Molecular Oncology Group, Lady Davis Institute for Medical Research,[1] and Departments of Microbiology and Immunobiology[3] and Medicine,[2] McGill University, Montreal, Quebec, Canada H3T 1E2

Received 14 August 2001/Accepted 16 January 2002

The mechanisms of cellular recognition for virus infection remain poorly understood despite the wealth of information regarding the signaling events and transcriptional responses that ensue. Host cells respond to viral infection through the activation of multiple signaling cascades, including the activation of NF-κB, c-Jun/ATF-2 (AP-1), and the interferon regulatory factors (IRFs). Although viral products such as double-stranded RNA (dsRNA) and the processes of viral binding and fusion have been implicated in the activation of NF-κB and AP-1, the mechanism(s) of IRF-1, IRF-3, and IRF-7 activation has yet to be fully elucidated. Using recombinant measles virus (MeV) constructs, we now demonstrate that phosphorylation-dependent IRF-3 activation represents a novel cellular detection system that recognizes the MeV nucleocapsid structure. At low multiplicities of infection, IRF-3 activation is dependent on viral transcription, since UV cross-linking and a deficient MeV containing a truncated polymerase L gene failed to induce IRF-3 phosphorylation. Expression of the MeV nucleocapsid (N) protein, without the requirement for any additional viral proteins or the generation of dsRNA, was sufficient for IRF-3 activation. In addition, the nucleocapsid protein was found to associate with both IRF-3 and the IRF-3 virus-activated kinase, suggesting that it may aid in the colocalization of the kinase and the substrate. Altogether, this study suggests that IRF-3 recognizes nucleocapsid structures during the course of an MeV infection and triggers the induction of interferon production.

The success of the innate host defense to viral infection is dependent on the ability of the cell to detect the presence of the invading pathogen. Upon recognition, the cell initiates a multitude of signal transduction cascades that produce protein messengers in the form of cytokines (for a review, see reference 43). Essential components of the cytokine host defenses are the family of transcriptionally activated, secreted proteins termed interferons (IFNs), which include alpha/beta IFN (IFN-α/β) and IFN-γ. IFN-α/β can be further subdivided into two groups: immediate-early genes (IFN-β and IFN-α1), which do not require de novo synthesis of proteins, and delayed-type IFN genes, which are induced through the upregulation of transcription factors produced following the immediate-early response (33, 44).

The rapid induction of IFN-α/β immediate-early genes requires posttranslational modifications of the transcription factors involved in immunomodulation. Phosphorylation events induce the activation of ATF-2/c-Jun (AP-1) (12) and the nuclear accumulation of both NF-κB (10) and interferon regulatory factor 3 (IRF-3) (25, 28, 37, 54, 57), which permit the formation of a ternary complex structure on the IFN-β promoter termed the enhanceosome (13, 23, 35, 53, 54). Recent knockout studies have demonstrated that the IFN-β response to viral infection was dramatically reduced in the absence of IRF-3 (44). IRF-1, like IRF-3, is capable of binding to the IFN-β promoter (26, 36), but unlike IRF-3, IRF-1 null mice showed normal expression of IFNs following viral infection (34, 41).

IRF-3 is a 427-amino-acid phosphoprotein that is constitutively expressed in two forms (I and II) of about 55 kDa when resolved by sodium dodecyl sulfate-polyacrylamide gel electrophoresis (SDS-PAGE) (28, 48). Upon viral infection, IRF-3 is phosphorylated within the C terminus of the protein on serines 385 and 386 (57) but also on serine residues 396, 398, 402, and 405 and threonine 404 (28), which will induce phosphorylated forms III and IV, which migrate more slowly on SDS-PAGE (48). C-terminal phosphorylation causes a conformation change in the protein that reveals both the IRF association domain and the DNA binding domain, permitting dimerization and binding to IRF DNA consensus sites (28, 57). In addition, IRF-3 C-terminal phosphorylation permits association with the histone acetyltransferase nuclear proteins CBP and p300 (28, 57), causing IRF-3, which normally shuttles in and out of the nucleus, to become predominantly nuclear (25, 28, 57). This active form of IRF-3, bound to CBP, is capable of inducing transcription through distinct positive regulatory domains or through select interferon-stimulated response elements (ISREs) (28, 30, 46, 54, 55, 57). Finally, IRF-3 is degraded through a proteosome-mediated mechanism (28, 42).

The virus-activated kinase responsible for IRF-3 phosphorylation has yet to be identified, although pharmacological and molecular studies suggest that it is a novel serine/threonine kinase activated in response to a variety of viral infections (48, 49). Virus-activated kinase represents a component of the cellular machinery that recognizes the viral pathogen and, like the IκB kinase and the c-Jun amino-terminal kinases, activates transcription factors involved in the immediate-early response to viral infection (9).

* Coresponding author. Mailing address: Lady Davis Institute for Medical Research, 3755 Cote St. Catherine, Montreal, Quebec H3T 1E2, Canada. Phone: (514) 340-8222. Fax: (514) 340-7576. E-mail: jhisco@po-box.mcgill.ca.

A variety of studies identifying viral activators of IRF-3 has shown that Sendai virus, measles virus (MeV), Newcastle disease virus, vesicular stomatitis virus, respiratory syncytial virus, sin nombre virus, and Hantaan virus activate IRF-3 during the course of infection (7, 37, 48, 51). The fact that this list is biased towards closely related, single-stranded, enveloped RNA viruses suggested that the IRF-3 cascade was limited to viral RNA detection and that activation of virus-activated kinase may be due to a component of the viral life cycle.

A number of studies on IRF-3 activation suggested a role for double-stranded RNA (dsRNA) (21, 54, 55, 57), a by-product of viral replication that is known to activate the dsRNA-activated kinase PKR. However, studies in PKR null cells as well as null cells of other PKR-like family members failed to abrogate IRF-3 phosphorylation (49, 55). In addition, two novel viral activators for IRF-3 have been identified which, unlike those characterized previously, are DNA viruses. Human cytomegalovirus and herpes simplex virus type 1 have both been found to induce IRF-3 activation even in the presence of actinomycin D, when no viral RNA is produced (39), providing further evidence that IRF-3 activation may require an alternative component of the virus life cycle.

To investigate which component(s) of the viral life cycle is required for IRF-3 phosphorylation, a genetic approach was used with recombinant MeV components. We demonstrate that IRF-3 activation is dependent on replication at a low multiplicity of infection (MOI), when defective interfering particles should not be a significant factor. The viral nucleocapsid (N) protein was identified as the major component of IRF-3 activation. N protein alone induces IRF-3 phosphorylation in a concentration-dependent manner and in stable cells expressing N protein. In addition, the C-terminal domain of N was found to associate with IRF-3 through its IRF association domain in addition to having the ability to associate with the virus-activated kinase itself. Together, these results indicate that the N protein is directly recognized by IRF-3, resulting in IRF-3 phosphorylation, nuclear translocation, and transcriptional activation.

MATERIALS AND METHODS

Cell culture, transfections, and reagents. HEC1B, HEK293, HEK293 Flag-N, and 293-3-46 cells were maintained in Dulbecco's modified Eagle's medium supplemented with 10% fetal bovine serum, nonessential amino acids, L-glutamine, sodium pyruvate, and selection reagents where applicable. The human lung carcinoma cell line A549 was maintained in F12K medium supplemented with 10% fetal bovine serum. pcDNA3.1 Zeo Flag-N was transfected into HEK293 cells and selected in the presence of 100 μg of zeocin (Invitrogen) per ml to obtain a stable monoclonal population. The 293-3-46 cell line has been described previously and was maintained in the presence of 400 μg of G418 (Gibco) per ml (40). All transfections of 293 cell lines, both parental and stable, were performed using the calcium phosphate method.

Cloning. MeV cDNA clones were a gift from M. A. Billeter and have been described elsewhere (47). The pSC-nucleocapsid wild-type cDNA was subcloned using specific primers containing forward *Not*I and reverse *Bgl*II cloning linker sites, 5′-AGGTCGGCCGCTCATCCAATGTCCATCATGGG-3′ and 5′-AGGTAGATCTAGGAGACTTGTGGGACATTTG-3′, respectively. Nucleocapsid N-terminal mutants were made using the identical template and forward primer with the following reverse primers: N1-366 (5′-CTACTATGACCTCCTTACCATCTCTT-3′) and N1-415 (5′-CTACTATGATACTTGGGCTTGTCTG-3′). The C-terminal N mutant was constructed with an internal forward primer (5′-GCGGACCAATACTTTTCACAT-3′) and the wild-type reverse primer mentioned previously. PCR products were cloned into a modified pcDNA3.1 (Invitrogen) containing a Flag epitope just prior to the multicloning site. All IRF-3 constructs used have been described previously (29).

Viral infections. MeV (Edmonston strain) was added to serum-free medium in minimal volume at a multiplicity of infection of 1.0. Sendai virus infections were performed in an identical manner at a concentration of 25 hemagglutinating units (HAU)/10^6 cells. After 2 h of incubation, complete medium was added for the duration of the infection.

Rescue of MeV. The use of recombinant cDNAs to rescue MeV replication was performed as described previously (40). Briefly, 293-3-46 cells expressing T7 polymerase, N, and P MeV proteins were transfected with the L polymerase gene of MeV and the full-length positive-strand genome encoded in pBluescript (MV+NSE). At 24 h posttransfection, the medium from the 293-3-46 was transferred onto A549 cells consecutively every 6 h for 72 h; cells were then lysed for whole-cell extract preparation with NP-40 lysis buffer. The production of MeV lacking a functional L polymerase was accomplished by removing 1,000 bp from the L gene through an *Afl*II restriction digest of the wild-type (MV+NSE) genome and complemented in the packaging 293-3-46 cells with wild-type L polymerase.

Immunoblot analysis. To investigate the phosphorylation state of IRF-3, whole-cell extracts from the various cell lines were subjected to SDS-PAGE in a 7.5% polyacrylamide gel. Following electrophoresis, the proteins were transferred to a Hybond-C transfer membrane (Amersham) in buffer containing 30 mM Tris, 200 mM glycine, and 20% methanol for 2 h at 50 V at 4°C. The membrane was blocked in 5% dried milk in Tris-buffered saline (TBS) plus 0.1% Tween 20 (TBST) for 1 h at room temperature and was then probed with polyclonal IRF-3 antibody (a gift from Paula Pitha, Johns Hopkins University) at a dilution of 1:5,000.

Immunoblots using measles whole virus (a gift from Brian Ward, McGill University), Flag (Sigma F3168), Myc (Sigma 9E10), IRF-1 (Santa Cruz SC-9082), IRF-7 (Santa Cruz SC-9083), and actin (Chemicon MAB1501) were immunoblotted under the same conditions using concentrations of 1 μg/ml unless otherwise stated. Incubations were done overnight at 4°C and washed in TBST five times for a total of 25 min. Following washes, the membrane was incubated with peroxidase-conjugated goat anti-rabbit immunoglobulin (Ig) antibody (Amersham) at a dilution of 1:5,000 for 1 h at room temperature. Following the incubation with the secondary antibody, the membrane was washed again for 25 min and then visualized with the enhanced chemiluminescence detection system as recommended by the manufacturer (Amersham Corp.)

Electrophoretic mobility shift assay. Cellular samples were washed in phosphate-buffered saline (PBS) and pelleted to obtain nuclear extracts. Briefly, pellets were treated with 10 mM HEPES, 50 mM NaCl, 10 mM EDTA, 5 mM $MgCl_2$, 0.5 mM spermidine, 0.15 mM spermine, 0.5 mM phenylmethylsulfonyl fluoride (PMSF), leupeptin (10 μg/ml), pepstatin (10 μg/ml), aprotinin (10 μg/ml), and 1 mM Na_3VO_4. The suspension was held on ice for 30 min and brought to 0.1% NP-40 and 10% glycerol concentration. Samples were spun for 5 min at 5,000 rpm at 4°C. Supernatant was removed, and the pellet was washed in 50 mM NaCl. Nuclear extracts were obtained in a 10 mM HEPES–400 mM NaCl–0.1 mM EDTA–0.5 mM dithiothreitol–0.5 mM PMSF–leupeptin (10 μg/ml)–pepstatin (10 μg/ml)–aprotinin (10 μg/ml)–1 mM Na_3VO_4 solution. Samples were left to rotate at 4°C for 30 min and spun at 15,000 rpm for 10 min at 4°C.

Equivalent amounts of HEK293 nuclear extracts were assayed for IRF-3 binding in a gel shift analysis using a ^{32}P-labeled double-stranded oligonucleotide corresponding to the interferon-stimulated response element of the inducible ISG15 gene (5′-GATCGGAAAGGGAAACCGAAACTGAAGCC-3′). Complexes were formed by incubating the probe with 10 μg of nuclear extract for 20 min at room temperature in 10 mM Tris-Cl (pH 7.5)–1 mM EDTA–50 mM NaCl–2 mM dithiothreitol–5% glycerol–0.5% Nonidet P-40–1 μg of bovine serum albumin (BSA) per μl–poly(dI-dC) (1.0 μg/μl). Extracts were run on a 5% polyacrylamide gel (60:1 cross-link) prepared in 0.25× Tris-borate-EDTA (TBE). After running at 160 V for 3 h, the gel was dried and exposed to a Kodak film at −70°C overnight. To demonstrate the specificity of the detected signal, 1 μg of anti-IRF-3 (Santa Cruz FL-425) or anti-CBP (Santa Cruz SC-369X) antibody was incubated for 30 min on ice prior to the addition of the probe to observe a supershift in the complex formation.

UV cross-linking. UV inactivation of MeV was performed using the Stratagene Stratalinker. MeV at an MOI of 1.0 in cell culture medium was exposed for 0, 30, and 60 s of UV cross-linking prior to application onto A549 cells.

In vitro kinase assay. IRF-3 kinase activity was assayed by incubating whole-cell extract (2 μg) or bound protein from the Flag-IRF-3/Flag-N 4-h immunoprecipitation in a total volume of 40 μl of kinase assay buffer (50 mM Tris [pH 7.5], 2 mM $MgCl_2$, and 2 mM $MnCl_2$) containing 1 μg of both recombinant C-terminal glutathione *S*-transferase–IRF-3 (GST–IRF-3, amino acids 380 to 427) protein and GST alone, 10 μM ATP, and 10 μCi of [γ-^{32}P]ATP. The reaction was initiated by the addition of ATP, incubated at 30°C for 45 min, and stopped with the addition of 2× denaturing sample buffer. The samples were

analyzed by SDS gel electrophoresis on 12% acrylamide gels. Dried gels were exposed to Kodak films at −70°C for 1 h.

Additional kinase assays performed on immunoprecipitated extract were done with Flag-N and Flag-IRF-3; 30 μl of protein G was precoupled with 2 μg of Flag antibody in 50 mM Tris, 150 mM NaCl, 5 mM EDTA, and 0.1% Triton X-100 (TNET) and 1% BSA for 2 h at 4°C. Following this, 1 mg of whole-cell extract was incubated with the slurry overnight, followed by five washes in NP-40 lysis buffer. The kinase assay itself was performed as described above in the presence of the beads and anything that remained associated with the Flag constructs.

Luciferase assays. All transfections were carried out on subconfluent HEK293 cells grown in six-well plates. A total of 2 μg of DNA constructs (per well) and 10 ng of pRL null reporter (*Renilla* luciferase for internal control) were introduced into target cells. At 12 h posttransfection, cells were infected with MeV (MOI = 1.0). At 36 h, cells were collected, washed in ice-cold phosphate-buffered saline, and assayed for reporter gene activity as described by the manufacturer (Promega). Reporter constructs included the RANTES promoter and the NF-κB-responsive promoter P2 (2) and are described elsewhere (48).

RPA. The 293 IRF-3ΔN- or 293 IRF-3 wild-type-expressing cells were either left untreated or infected with MeV (MOI = 1) for 72 h. Total RNA was prepared from the cell pellets using the Qiagen RNeasy kit. A total of 5 μg of RNA was subjected to RNase protection assay (RPA) using the hCK-5 chemokine template of the RiboQuant multiprobe RPA kit, following the manufacturer's instructions (Pharmingen).

Two-dimensional electrophoresis. A total of 10^6 ATCC 293 cells were harvested 36 h posttransfection and lysed in 500 μl of 3-[(3-cholamidopropyl)-dimethylammonio]-1-propanesulfonate (CHAPS) lysis buffer for 1 h at room temperature. Then 100 μg of protein sample was incubated with 0.5% immobilized pH gradient (IPG) buffer and Orange G dye and completed to 250 μl with lysis buffer before being added to 13-cm IPG strips (pH 3 to 10). Samples were hydrated for 12 h, followed by three sequential steps of 500 V for 1 h, 1,000 V for 1 h, and 8,000 V for 4 h. Migration was performed using the IPGphor (Pharmacia) before being transferred to the second-dimension Western blot apparatus. The stacking gel was replaced with a 1% low-melting-point agarose in stacking buffer containing bromophenol blue at 0.01%. Following electrophoresis, samples were transferred and blotted as described in the immunoblot analysis section using a polyclonal antibody to IRF-3 (Santa Cruz SC-9082).

Immunoprecipitation. For coprecipitation studies, whole-cell extract (500 μg) was incubated with 1 μg of anti-Flag (Sigma) or anti-IRF-3 (SC FL-425) cross-linked to 30 μl of protein G- and protein A-Sepharose beads, respectively, for 3 h at 4°C (Amersham Pharmacia). The beads were washed five times with Nonidet P-40 lysis buffer and resuspended in denaturing sample buffer, and the eluted IRF-3 or N proteins were analyzed by immunoblotting.

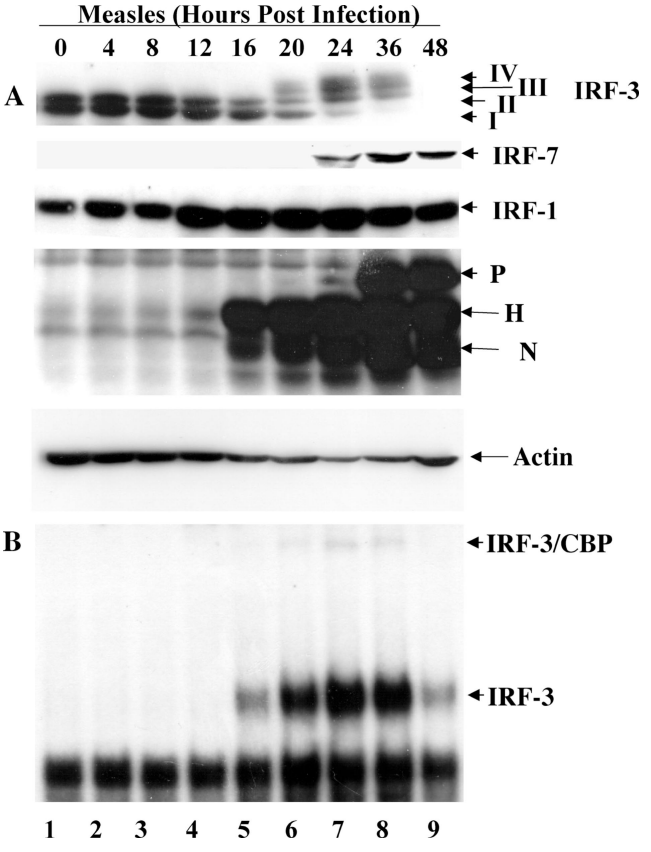

FIG. 1. Activation of IRFs following MeV infection in A549 cells. (A) Whole-cell extract (100 μg) prepared from A549 cells infected with MeV (MOI = 1.0) for different periods of time was resolved by SDS–7.5% PAGE and transferred to nitrocellulose. IRF-3 (forms I to IV), IRF-7, IRF-1, MeV proteins, and actin were detected by immunoblotting. MeV phosphoprotein, hemagglutinin protein, and nucleocapsid protein are denoted P, H, and N, respectively. (B) Nuclear extracts were collected from duplicate experiments as outlined above and used to analyze IRF-3 binding activity by electrophoretic mobility shift assay using the ISRE of ISG15 as the probe. Arrows indicate complexes of IRF-3 and IRF-3/CBP.

RESULTS

IRF activation by MeV in A549 cells. Previous studies have demonstrated that MeV (Edmonston strain) of the *Paramyxoviridae* family induced the phosphorylation and activation of IRF-3 in HEC1B and A549 cells (48). To further investigate IRF activation, A549 cells were infected with MeV at an MOI of 1.0 and harvested at various times from 0 to 48 h postinfection (h.p.i.); whole-cell extracts were specifically immunoblotted with antisera against IRF-3, -7, and -1, actin, and whole MeV serum. IRF-3 phosphorylation is relatively easy to detect in extracts from virus-infected cells because it migrates more slowly in SDS-PAGE than the nonphosphorylated forms and is subject to proteasome-mediated degradation (28, 42, 48, 55, 57).

C-terminal phosphorylation following MeV infection, detected as forms III and IV (48), was observed between 20 and 36 h.p.i., followed by IRF-3 degradation (Fig. 1A, lanes 6 to 9). The induction of IRF-7 in response to MeV infection occurred following IRF-3 phosphorylation and was detected at 24 to 48 h.p.i. (Fig. 1A, lanes 7 to 9). In contrast, IRF-1 production was induced as early as 12 h.p.i. and was maintained for the duration of the infection (Fig. 1A, lanes 4 to 9). MeV replication appeared to correlate well with the onset of IRF activation, since the hemagglutinin (H) and nucleocapsid (N) proteins were detected at 16 h.p.i. and the phosphoprotein (P) at 24 h.p.i. (Fig. 1A, lanes 5 and 7).

As a further measure of IRF-3 activation, IRF-3 DNA binding activity was analyzed by electrophoretic mobility shift assay using the ISRE of the ISG15-responsive gene as a probe. IRF-3 C-terminal phosphorylation, as represented by forms III and IV (Fig. 1A, lanes 6 to 9), correlated with the ability of IRF-3 to bind DNA; two specific complexes representing IRF-3 and CBP bound to DNA were identified. Binding was detected at 16 h.p.i. and was maintained for the duration of the infection (Fig. 1B, lanes 5 to 9), suggesting that the electrophoretic mobility shift assay represents a more sensitive assay than SDS-PAGE. The inducible complexes were shown to be IRF-3 and IRF-3/CBP by competitive supershift analysis using IRF-3- and CBP-specific antibodies (data not shown). These data demonstrate that MeV infection induces the phosphorylation of IRF-3 and upregulation of IRF-1 and IRF-7 during the course of infection.

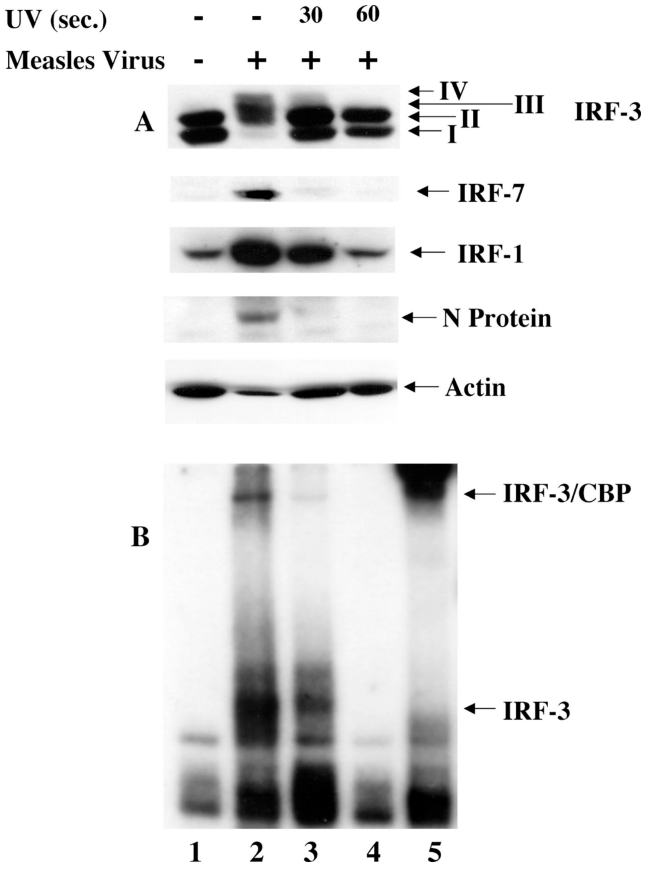

FIG. 2. IRF-3 activation requires viral transcription. (A) MeV stocks were UV treated for 0, 30, or 60 s and added to target A549 cells at an MOI of 1.0 for 24 h. Whole-cell extract (75 μg) was prepared and run on SDS–7.5% PAGE. Endogenous proteins were detected by immunoblotting with IRF-3, IRF-7, IRF-1, MeV N, and actin antibodies. (B) Nuclear extracts were prepared from duplicate experiments as outlined above and used to analyze IRF-3 DNA binding activity by electrophoretic mobility shift assay using the ISRE of ISG15 as the probe. Arrows indicate complex formation of IRF-3 and IRF-3/CBP as determined by supershift of these complexes (IRF-3 supershift, lane 5; CBP supershift, data not shown).

IRF-3 activation requires viral transcription. Next, to determine if the events of MeV transcription were required for IRF-3 activation, an MeV virion stock was subjected to UV cross-linking (see Materials and Methods) (11). Following 0, 30, and 60 s of UV cross-linking, original MeV titers (MOI = 1.0) were used to infect A549 cells. At 24 h.p.i., whole-cell extract was harvested and specifically immunoblotted for IRF-3, -7, and -1, MeV proteins, and actin. Following 30 s of UV cross-linking, IRF-3 phosphorylation in response to MeV infection was diminished more than 80% compared to untreated virus (Fig. 2A, lanes 2 and 3). Furthermore, activation was completely abrogated after 60 s of UV cross-linking, suggesting that viral transcription was required for IRF-3 phosphorylation (Fig. 2A, lane 4).

Likewise, IRF-7 induction was only detected after 24 h using untreated-virus infection (Fig. 2A, lane 2). In addition, IRF-1 induction appeared to be dependent on viral transcription, with a 3.4-fold upregulation upon 30 s of UV cross-linking, compared to 6.2-fold induction in the absence of cross-linking (Fig. 2A, lanes 2 and 3). This activation was completely abrogated in the MeV stock treated for 60 s with UV inactivation (Fig. 2A, lane 4). Inhibition of viral transcription after cross-linking was confirmed by the absence of the virus-specific nucleocapsid protein in the UV-treated extracts (Fig. 2A, lanes 2 to 4), in addition to Northern blot analysis for the presence of MeV RNA (data not shown).

To confirm that IRF-3 activation was dependent on viral transcription, an electrophoretic mobility shift assay was performed using the ISRE of the ISG15 promoter. As shown in Fig. 1, binding of IRF-3 and CBP correlated with the appearance of forms III and IV (Fig. 2B, lane 2). Binding was detected in the absence of UV cross-linking, with minimal binding following 30 s (Fig. 2B, lanes 2 and 3) of UV inactivation, whereas after 60 s of UV inactivation, the DNA binding activity of IRF-3 was completely eliminated (Fig. 2B, lane 4).

The specificity of the electrophoretic mobility shift assay complexes was confirmed through the use of an IRF-3 antibody to supershift the inducible complexes (Fig. 2B, lane 5). The higher-migrating complex was confirmed to contain CBP by supershift analysis (data not shown). Taken together, these data show that transcription is required for the phosphorylation of IRF-3 and the induction of IRF-1 and IRF-7. Furthermore, as previously demonstrated for Sendai virus (48), the RNA polymerase inhibitor ribavirin also blocked IRF-3 phosphorylation and activation in MeV-infected cells (data not shown).

IRF-3 activation requires a functional MeV polymerase. To further investigate the requirement for MeV replication in IRF-3 activation, a reverse genetics approach was used to rescue MeV production from cloned MeV DNA containing a 1,000-bp deletion in the large (L) polymerase. Briefly, using a strategy described previously (40), stable 293-3-46 cells, which express T7 polymerase, the nucleocapsid (N) protein, and the phosphoprotein (P), were transfected with the wild-type L polymerase, in addition to either the wild-type MeV cDNA genome or a genome containing a deletion in the L polymerase (ΔL). At 48 h posttransfection, supernatant containing pseudovirions was applied to target A549 cells every 6 h for an additional 48 h to ensure viral infection despite low titer production. Whole-cell extracts from infected target cells were specifically immunoblotted for IRF-3, -7, and -1, MeV protein, and actin (Fig. 3).

IRF-3 phosphorylation, as detected by the formation of forms III and IV, was observed with wild-type MeV, but was not observed during the rescue of the ΔL virus (Fig. 3A, lanes 1 to 3). Only wild-type MeV induced IRF-7 expression, although ΔL virus induced a weak 1.4-fold increase in IRF-7, perhaps as a result of IFN production in the 293-3-46 helper cells (Fig. 3A, lanes 2 and 3). IRF-1 induction was detected in both wild-type- and ΔL-infected cells, suggesting that its induction is dependent on an event prior to transcription that UV inactivation was capable of inhibiting (Fig. 2A) and suggests that similar virus titers were produced by the helper 293-3-46 cells upon transfection (Fig. 3A, lanes 2 and 3).

The same extracts were blotted against MeV serum and demonstrated the production of wild-type MeV proteins (Fig. 3A, lane 2), whereas only the hemagglutinin (H) receptor protein was detected in ΔL rescued virus extracts (Fig. 3A, lane 3). Electrophoretic mobility shift assay analysis also confirmed

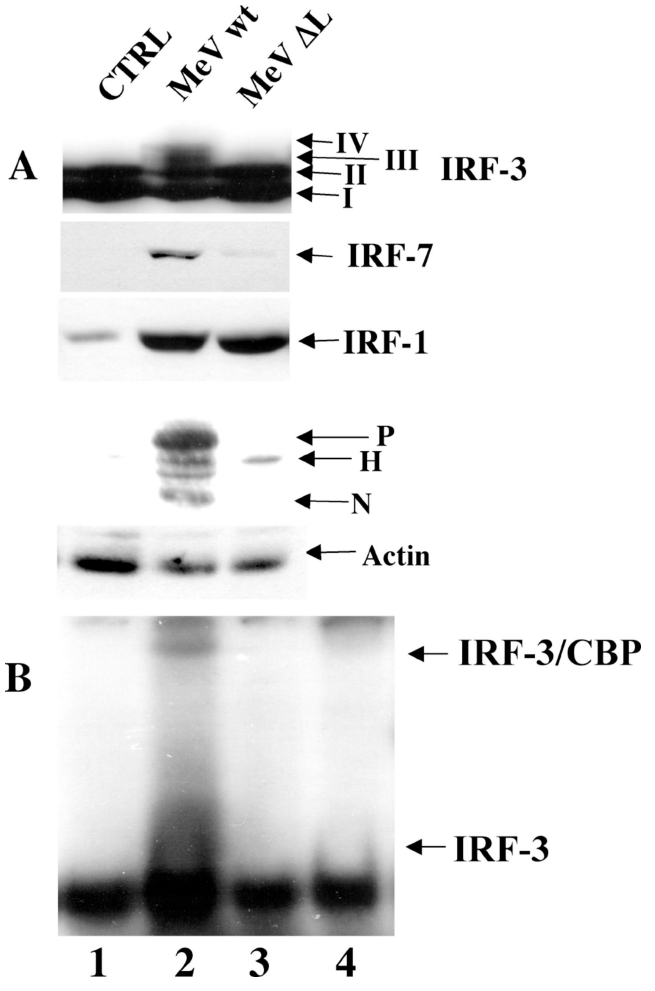

FIG. 3. IRF-3 activation requires a functional MeV polymerase. (A) Rescued MeV from wild-type cDNA (MeVwt) or cDNA encoding a truncated polymerase (MeVΔL) was produced in 293-3-46 cells and used to treat target A549 cells as described in the Materials and Methods section. At 72 h.p.i., cells were harvested and run on an SDS–7.5% PAGE gel. Endogenous proteins were detected in whole-cell extract (100 μg) by immunoblotting with IRF-3, IRF-7, IRF-1, MeV, and actin antibodies. (B) Nuclear extracts were collected from duplicate experiments as outlined above and used to analyze IRF-3 DNA binding activity by electrophoretic mobility shift assay using the ISRE of ISG15 as the probe. Arrows indicate complex formation of IRF-3 and IRF-3/CBP as determined by supershift of these complexes (IRF-3 supershift, lane 4; CBP supershift, data not shown).

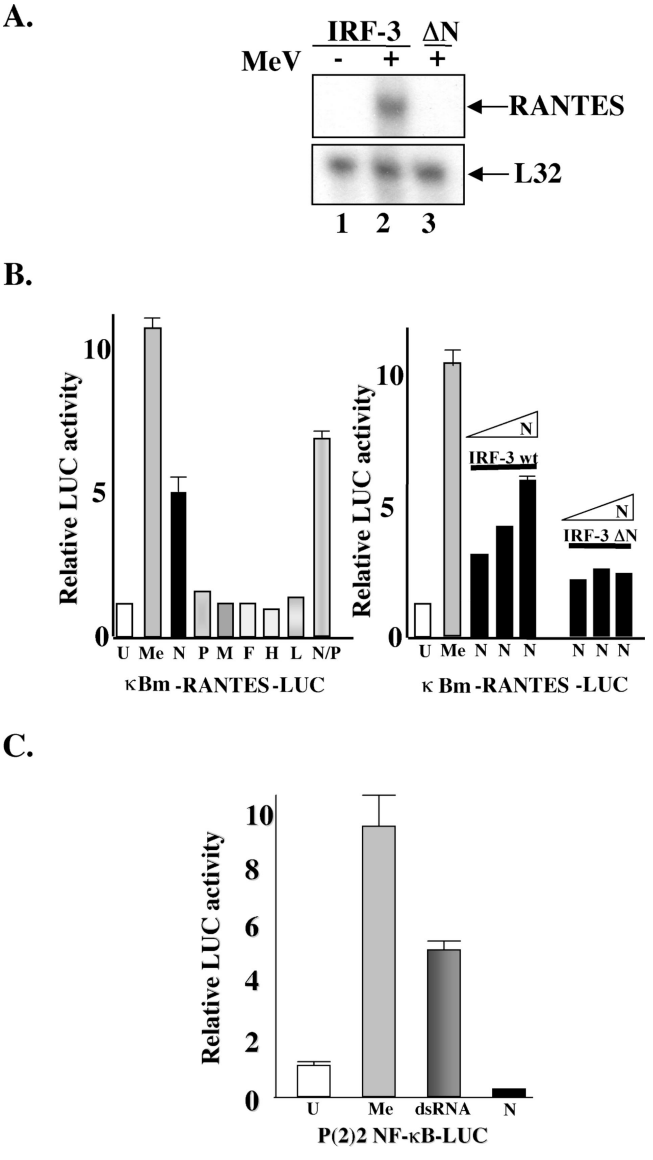

FIG. 4. RANTES induction by MeV and MeV N protein. (A) HEK293 cells expressing IRF-3 ΔN and IRF-3 wild-type were infected with MeV (MOI = 1.0) for 72 h. Total RNA (5 μg) was isolated and analyzed by RPA for the expression of RANTES and L32. (B) Left panel: HEK293 cells were transfected with the κB-mutated RANTES promoter (κBm-RANTES-LUC) reporter plasmids and MeV protein constructs as indicated. At 24 h posttransfection, cells were harvested, and relative luciferase (LUC) activity was measured as fold activation. Each value represents the mean ± standard error (SE) of triplicate determinations. Right panel: HEK293 cells were cotransfected with increasing concentrations of N cDNA (0.5 to 1.5 μg) in addition to a constant level of either IRF-3 wild-type or IRF-3 ΔN (1.0 μg). Experiment was performed as above. (C) HEK293 cells were transfected with the NF-κB-responsive promoter P2 (2) and either empty vector or N protein. Cells were treated with MeV (MOI = 1.0) or dsRNA (100 μg/ml) and harvested 36 h posttransfection, and relative luciferase activity was measured as fold activation. Each value represents the mean ± SE of quadruplicate experiments. The treatments and constructs used were: untreated (U), MeV (Me), nucleocapsid protein (N), phosphoprotein (P), matrix protein (M), fusion protein (F), hemagglutinin protein (H), large polymerase protein (P), and dsRNA.

that IRF-3 DNA binding activity was detected with wild-type virus (Fig. 3B, lane 2) but not with ΔL (Fig. 3B, lane 3). Specific complex formation was determined by supershift analysis with IRF-3 (Fig. 3B, lane 4) and CBP (data not shown). The reverse genetics approach further supports the notion that IRF-3 and IRF-7 activation requires a replication-competent virus.

IRF-3-dependent RANTES expression by MeV is mimicked by N protein. It has been demonstrated previously that MeV stimulates the production of the CC-chemokine RANTES in an MOI-dependent fashion in astrocytes (38). To investigate the requirement for IRF-3, a 293 cell line expressing dominant negative ΔN IRF-3 (which lacks the DNA binding domain of

IRF-3) (18, 29) was infected with MeV (MOI = 1.0); at 48 h.p.i., total RNA was isolated and analyzed by RPA.

In the presence of ΔN IRF-3, MeV failed to induce RANTES induction compared to the parental cell line (Fig. 4A, lanes 2 and 3), demonstrating that MeV-induced RANTES expression also required activation of IRF-3 (15). Since activation of IRF-3 was found to be dependent on the replication state of MeV, we hypothesized that an MeV protein may be involved in the induction of RANTES. To determine if MeV viral proteins were necessary, each of the seven major MeV proteins was expressed in a luciferase reporter assay using the RANTES promoter in which the two NF-κB sites were mutated, rendering the promoter responsive only to IRF-3 (27). In agreement with the published literature (38), only N protein or N in combination with P induced 5- and 7.2-fold inductions, respectively, of the IRF-3-dependent RANTES promoter (Fig. 4B, left panel). To ensure that this activation was dependent on IRF-3, N protein was coexpressed with wild-type IRF-3 or ΔN IRF-3; N protein induced RANTES activity with wild-type IRF-3 in a concentration-dependent manner, and this activity was blocked in the presence of ΔN IRF-3 (Fig. 4B, right panel).

Previous literature regarding IRF-3 activation has implicated dsRNA (55). To determine if N protein was inducing the production of dsRNA to activate IRF-3, an NF-κB-responsive luciferase assay was performed, as NF-κB has been well documented for its ability to be activated in response to dsRNA (9). Although both MeV and the synthetic dsRNA compound poly(I:C) were capable of inducing NF-κB activity 9.2- and 4.3-fold, respectively, nucleocapsid expression did not induce NF-κB-dependent reporter gene activity, but rather produced a slight repression in NF-κB activity (Fig. 4C). These data demonstrate that N protein is involved in the IRF-3-dependent induction of RANTES by MeV and that this activation is independent of dsRNA formation.

Expression of N protein induces the phosphorylation of IRF-3. Since N protein induced IRF-3 activation in a concentration-dependent manner as measured by luciferase assays, we investigated whether N could induce IRF-3 C-terminal phosphorylation. Using increasing amounts of Flag-tagged N (Flag-N) cotransfected with Myc-IRF-3, the induction of IRF-3 form III was detected at 48 h posttransfection (Fig. 5A, lane 5). As form IV was undetectable by one-dimensional SDS-PAGE analysis, a two-dimensional analysis was performed to investigate if the modification of IRF-3 in response to N was indeed comparable to that observed using the known viral activators of IRF-3. Two-dimensional analysis of extracts that were cotransfected with Flag-N and Myc-IRF-3 showed that the phosphorylation pattern of IRF-3 in response to N was indeed the same as that seen during a Sendai virus infection (Fig. 5B, compare middle panel to the bottom panel).

To further characterize N protein-induced IRF-3 phosphorylation, two stable cell lines, one expressing Flag-N alone and the other expressing both nucleocapsid (N) and phosphoprotein (P), were transfected with Flag-IRF-3; after 36 h of transfection, whole-cell lysates from these two N-expressing cell lines were immunoblotted with specific antibodies to Flag, IRF-7 and IRF-1 and compared with control 293 parental cells. IRF-3 phosphorylation was detected in both N-expressing cell lines compared to parental 293 cells (Fig. 5C, lanes 2 and 4). In addition, IRF-3 phosphorylation correlated with IRF-7 induction, whereas IRF-1 levels remained relatively unchanged. To ensure that this phosphorylation could be further correlated with IRF-3 activation, electrophoretic mobility shift assay analysis was performed, which demonstrated that both the Flag-N and the 293-3-46 stable cell lines were capable of inducing IRF-3 binding activity (Fig. 5D, lanes 2 and 5). The identity of

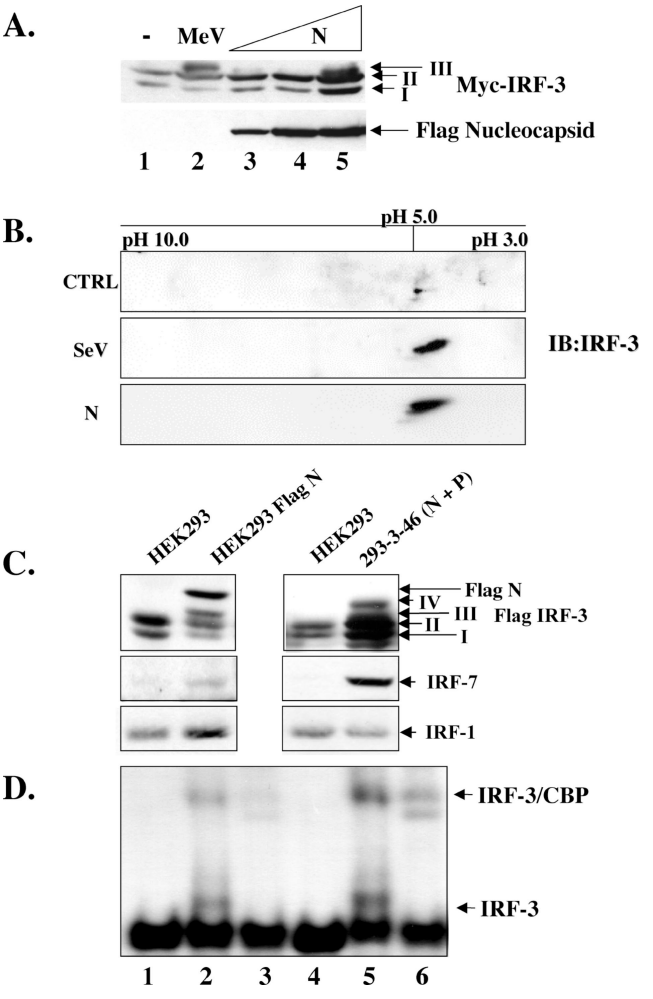

FIG. 5. Nucleocapsid protein alone induces IRF-3 phosphorylation. (A) HEK293 cells in 10-cm plates were cotransfected with Myc-IRF-3 (5 μg) and increasing amounts of Flag-N (5 to 15 μg; lanes 3 to 5). At 36 h posttransfection or 24 h.p.i. with MeV (MOI = 1.0), whole-cell extract (15 μg) was run on SDS–7.5% PAGE and analyzed by immunoblots using Flag and Myc antibodies. The positions of IRF-3 forms I, II, and III are indicated. (B) HEK293 cells in 10-cm plates were cotransfected with empty vector or Flag-N and Myc-IRF-3. Sendai virus (SeV) infection was performed at 25 HAU/10^6 cells for 10 h. At 36 h posttransfection, cells were harvested and subjected to two-dimensional electrophoresis. Shifts to the right imply phosphorylation events. (C) Stable cells expressing Flag N or untagged N and P (293-3-46) were transfected with Flag-IRF-3 (5 μg). At 36 h posttransfection, whole-cell extract (15 μg) was run on SDS–7.5% PAGE and analyzed by immunoblot using Flag antibody. Immunoblots for IRF-1 and IRF-7 were determined from whole-cell extract (80 μg) run on SDS–10% PAGE. (D) Nuclear extracts were collected from duplicate experiments as outlined above and used to analyze IRF-3 DNA binding activity by electrophoretic mobility shift assay using the ISRE of ISG15 as the probe. Arrows indicate complex formation of IRF-3 as determined by supershift analysis (IRF-3 supershift, lanes 3 and 6; CBP supershift, not shown).

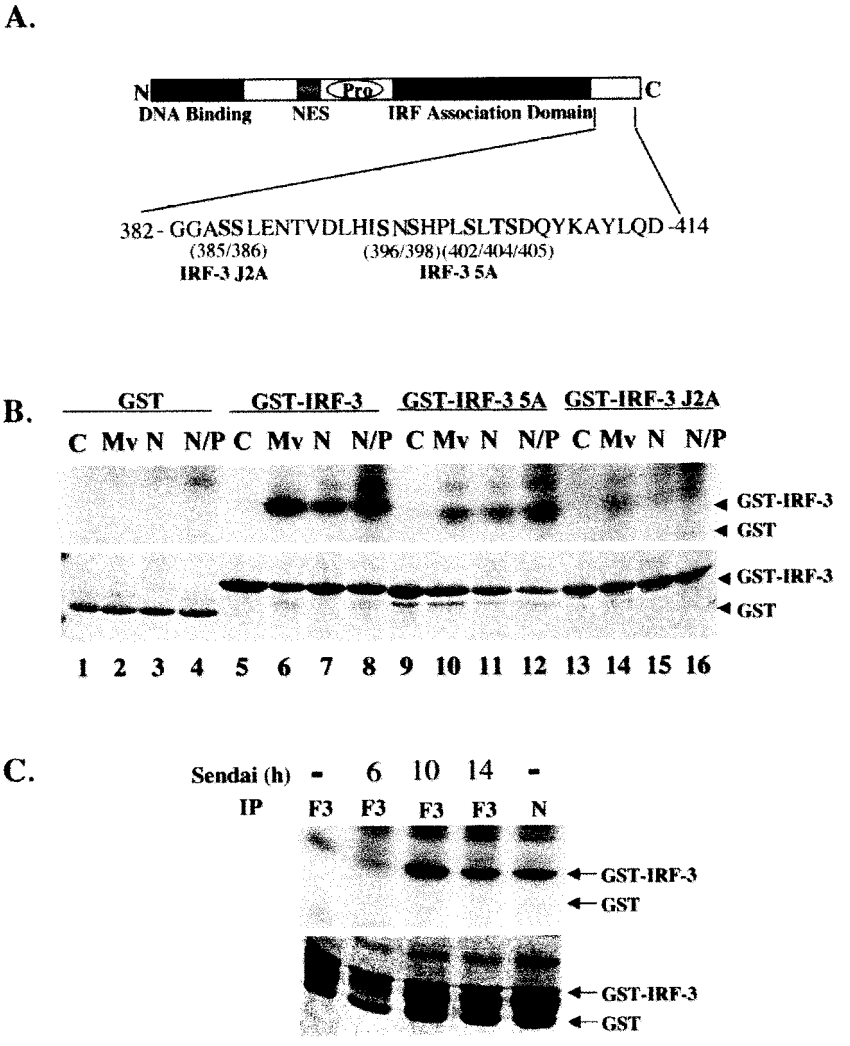

FIG. 6. Nucleocapsid protein induces and associates with the virus activated kinase (VAK). (A) Schematic representation of IRF-3. The DNA binding domain, the nuclear export sequence element, the proline-rich region, and the C-terminal IRF association domain are indicated. The region between amino acids 382 and 414 is expanded below the schematic in a depiction of IRF-3 C-terminal phosphorylation sites. The construct with serines 385 and 386 mutated to alanine has been denoted IRF-3 J2A. Residues 396, 398, 402, 404, and 405 mutated to alanine have been denoted IRF-3 5A. (B) Whole-cell extract (2 μg) derived from uninfected (−), MeV-infected at 24 h.p.i. at an MOI of 1.0 (Mv), and the stable Flag-N (N) and 293-3-46 (N/P) cell lines were used in an in vitro kinase assay using GST, GST–IRF-3 wild-type, GST–IRF-3 5A, and GST–IRF-3 J2A as substrates In all cases the IRF-3 moiety of the substrate spanned amino acids 380 to 427. Kinase reactions were run on SDS–12% PAGE, stained with Coomassie, dried, and exposed for 1 h at −70°C on an autoradiographic film. (C) HEK293 cells transfected with Flag-IRF-3 or Flag-N and harvested 36 h posttransfection. Sendai virus (SeV) infections were performed at the time points indicated. Whole-cell extract (1 mg) was incubated with protein G and Flag antibody overnight, and a kinase assay was performed as described for panel B with what was retained following the washes.

the inducible complex was confirmed through the addition of IRF-3 antibody (Fig. 5D, lanes 3 and 6). Taken together, these results demonstrate that N protein expression is capable of inducing IRF-3 phosphorylation and DNA binding activity.

Characterization of IRF-3 phosphorylation mediated by the MeV N protein. Next, the ability of N protein expression to stimulate the virus-activated kinase activity was evaluated, compared to the capacity of MeV to stimulate virus-activated kinase. Figure 6A illustrates the regulatory phosphorylation sites involved in IRF-3 activation, including Ser 385 and 386 and the serine/threonine cluster at Ser 396/398/402/405 and Thr 404 (28, 57). Alanine point mutations in Ser 385/386 are denoted as IRF-3 J2A, while the alanine substitutions in the Ser/Thr cluster are denoted as IRF-3 (5A). Virus-activated kinase activity in extracts from cell lines expressing N protein-induced phosphorylation of a GST–IRF-3 substrate (amino acids 380 to 427) (Fig. 6B, lanes 7 and 8), to a level comparable to the level observed with virus-activated kinase extracted from MeV-infected cells (Fig. 6B, lane 6). When the GST–IRF-3 (5A) substrate was used, the level of C-terminal phosphorylation by the virus-activated kinase was decreased 6.3-fold using extracts from MeV-infected or N-expressing cells (Fig. 6B, lanes 10 to 12).

Interestingly, phosphorylation was dramatically reduced

with the use of GST–IRF-3 J2A substrate (Fig. 6B, lanes 14 to 16), an observation that is consistent with previous observations suggesting that phosphorylation of serines 385 and 386 is essential for the sequential phosphorylation of the Ser/Thr cluster at amino acids 396 to 405. In addition to inducing the virus-activated kinase activity, the nucleocapsid protein was found to associate with the kinase, since immunoprecipitation assays retained kinase activity in the same manner as IRF-3 itself (Fig. 6C, lanes 3 to 5). This kinase activity was specific, as the profiles of IRF-3 5A and IRF-3 J2A phosphorylation were identical to those seen on the whole-cell extract kinase assays (data not shown). Taken together, these data suggest that N associates with virus-activated kinase and is capable of inducing its kinase activity.

N protein physically associates with IRF-3. One possibility to explain the ability of N protein to associate with and activate the virus-activated kinase was that N may physically associate with IRF-3 itself. To determine if the N protein interacted with IRF-3, the cell line expressing Flag-N was used to coimmunoprecipitate both Flag-N and endogenous IRF-3. This experiment showed that the basal levels of both proteins could be used to show an interaction as measured by coimmunoprecipitation (data not shown).

To define the domain of IRF-3 which physically associated with N, various Myc-IRF-3 deletion constructs were transfected into Flag-N-expressing cells, and coimmunoprecipitation was performed. IRF-3 was retained by Flag-N constructs expressing full-length IRF-3, IRF-3 lacking the C-terminal domain, and IRF-3 with an internal deletion, Δ134–197 (Fig. 7A, lanes 5, 6, and 8). IRF-3 was not immunoprecipitated by Flag-N when the truncated N-terminal (amino acids 1 to 197) region was used (Fig. 7A, lane 7). Thus, N interacts with IRF-3 in the region between amino acids 198 and 394, corresponding to the IRF association domain, as described previously (29).

In a reciprocal series of coexpression-immunoprecipitation experiments, full-length and deleted versions of Flag-tagged nucleocapsid were immunoprecipitated with Myc-tagged IRF-3 (Fig. 7B). Nucleocapsid deletions lacking the C-terminal domain of N (amino acids 1 to 366 and amino acids 1 to 415) were not immunoprecipitated with IRF-3 (Fig. 7B, lanes 6 and 7), whereas full-length nucleocapsid and an N-terminal deletion (amino acids 134 to 523) associated with IRF-3 (Fig. 7B, lanes 5 and 8), indicating that the region between amino acids 376 and 523 was required for nucleocapsid interactions with IRF-3. Thus, IRF-3 physically associates with MeV nucleocapsid in a complex that also contains the virus-activated kinase activity.

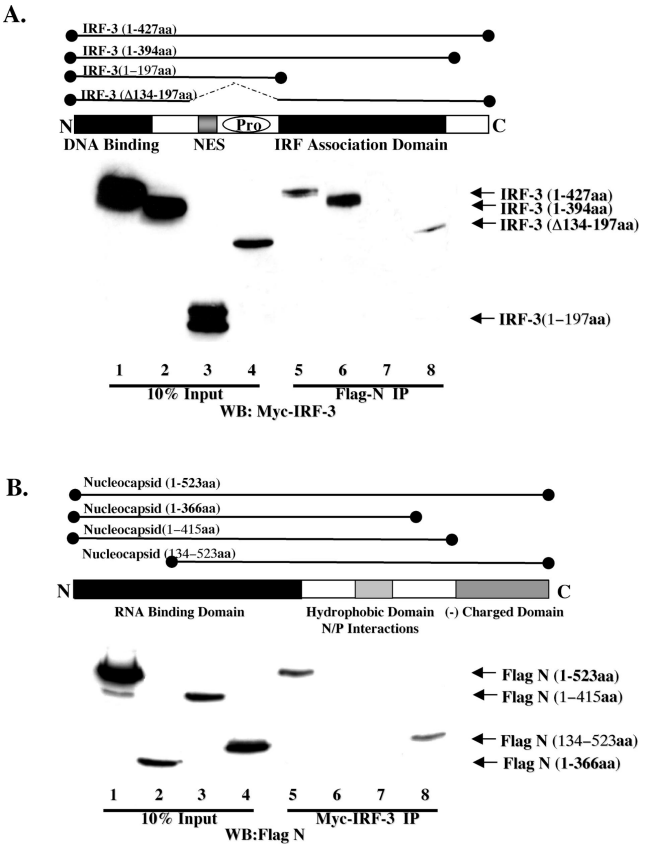

FIG. 7. Characterization of N and IRF-3 interaction. (A) HEK293 cells stably expressing Flag-N in 10-cm plates were transfected with various Myc-IRF-3 constructs encoding the various IRF-3 deletions depicted above in the schematic. Following immunoprecipitation of Flag-N, complexes were run on SDS–12% PAGE and immunoblotted using the anti-Myc antibody. Wild-type IRF-3 (amino acids 1 to 427; lanes 1 and 5), IRF-3 lacking the autoinhibitory domain (amino acids 1 to 394; lanes 2 and 6), IRF-3 lacking the IRF association domain (amino acids 1 to 197; lanes 3 and 7), and IRF-3 lacking the nuclear export sequence and proline-rich region (PRO) (Δ134–197; lanes 4 and 8) are depicted. The 10% input consisted of 50 μg of whole-cell extract (lanes 1 to 4). (B) HEK293 cells were cotransfected with Myc-IRF-3 and various Flag-N deletion constructs depicted in the schematic. Wild-type Flag-N (amino acids 1 to 523; lanes 1 and 5), two C-terminal deletions, Flag-N (amino acids 1 to 375; lanes 2 and 6) and Flag-N (amino acids 1 to 415; lanes 3 and 7), and an N-terminal mutant, Flag-N (amino acids 134 to 523; lanes 4 and 8), are depicted. The 10% input consisted of 50 μg of whole-cell extract (lanes 5 to 8).

DISCUSSION

The ability of the host cell to combat viral infection requires recognition of the incoming viral pathogen and subsequent induction of signaling cascades that culminate in the production of antiviral cytokines. IRF-3 plays an essential role in priming surrounding cells for an ongoing viral infection through the immediate-early induction of IFNs (22), the CC-chemokine RANTES (15, 27), and interleukin-15 (2). These secreted proteins serve to recruit cells of the host immune system to the site of infection and provide a means to eliminate infected cells.

As with many early response factors, the induction of IRF-3 relies on posttranslational C-terminal phosphorylation events. Essential phosphorylation sites were identified at serines 385 and 386 (57), as well as serines 396, 398, 402, and 405 and threonine 404 (28), mediated by an as yet unidentified virus activated kinase(s). These phosphorylation events are responsible for the conformational change which induces dimerization, cytoplasmic to nuclear translocation, binding to CBP/p300, and transcriptional activation by IRF-3 (28, 37, 45, 54, 55, 57).

In the present study, we investigated the mechanism by which the host cell recognizes MeV infection, leading to the activation of IRF transcription factors. By focusing on the components of MeV leading to IRF-3 phosphorylation, we

found that the MeV nucleocapsid (N) protein alone induced IRF-3 activation via the induction of a virus-activated kinase activity. Interestingly, N protein associates with the virus-activated kinase activity and physically interacts with the IRF association domain of IRF-3, implying that IRF-3 itself detects the viral pathogen via nucleocapsid recognition. In contrast, replication-deficient MeV, which was incapable of activating IRF-3 or -7, was able to induce IRF-1 expression, indicating that the pathways leading to IRF-3 and -7 activation may be distinct from the pathways that activate IRF-1.

Using a low multiplicity of infection of 1.0, induced IRF-3 phosphorylation was found to occur between 18 and 24 h.p.i., independent of IFN production, suggesting the requirement for viral replication. At low titers, IRF-1 induction appeared to precede IRF-3 phosphorylation, whereas at higher titers (MOI = 50) IRF-3 phosphorylation could be seen at 8 h.p.i. and preceded the induction of IRF-1 (data not shown). The requirement for viral transcription appeared to be a common requirement of both IRF-1 induction and IRF-3 phosphorylation. However, replication was only required for IRF-3 activation, since ribavirin (data not shown) and replication-defective recombinant MeV containing a truncation in the L polymerase failed to induce IRF-3 phosphorylation, but maintained the ability to induce IRF-1. These fundamental differences in IRF activation suggest that the activation of each factor may be induced by different mechanisms.

The life cycle of the paramyxoviruses following cellular binding and fusion is dependent on the self-encoded and -packaged polymerase, which is composed of two proteins, the L polymerase and the P protein (17). Together, this functional polymerase binds a 52-bp consensus site termed the leader sequence and begins the initial transcription of the 3′ nucleocapsid gene (19) (Fig. 8). Upon reaching the stop codon and polyadenylation signal of the N gene, the polymerase will either reinitiate the transcription of the following 3′ gene (P) or dissociate from the genome and reinitiate at the original leader sequence (8). In this way, the initial transcriptional events induce a protein gradient with the highest production of 3′ genes and the lowest for those at the 5′-most extremities (L) (step 1, Fig. 8) (4). As transcription continues, the accumulation of both the initial leader RNA sequence and the N protein itself induces the switch from transcription to replication through binding and stabilization of the polymerase and the genome itself (3). This stabilization is believed to prevent the dissociation of the polymerase upon reaching the 5′ end of each gene and allows for the production of readthrough transcripts that form the cRNA strand of positive polarity (step 2, Fig. 8) (5). Once transcribed, the positive strand can serve as a template for replication in the production of full-length negative-strand templates, which are encapsidated by approximately 2,600 N monomers and packaged as progeny virus (steps 3 and 4, Fig. 8) (24).

To determine the protein requirement for IRF-3 phosphorylation, cDNA clones of each MeV gene were expressed alone or in combination and assayed for IRF-3 phosphorylation. Initial studies found that the highest activation of IRF-3 occurred in the presence of both the N and P proteins, with moderate activity using N alone. Although initially thought to require both proteins for activation, it was later determined that the same phenomenon was observed with the presence of

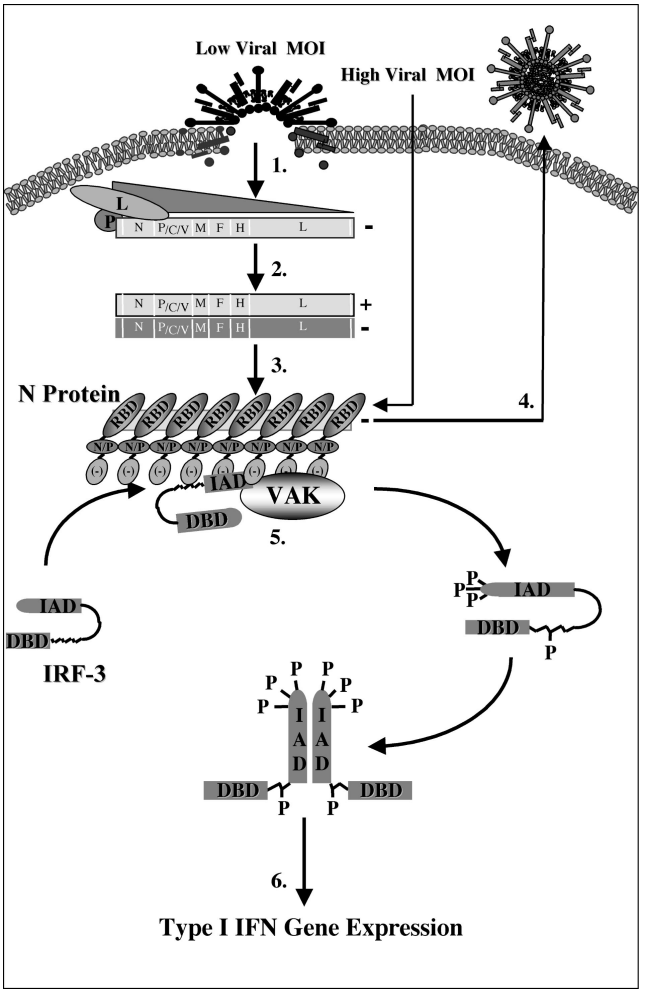

FIG. 8. Schematic representation of IRF-3 activation following MeV infection. Following viral binding and fusion, the genome of MeV is released into the cytoplasm in tight association with the nucleocapsid (N) protein. Upon entry, N dissociates from the negative-stranded template as it is transcribed by the packaged polymerase composed of both the large (L) and phospho- (P) proteins of MeV (step 1). Transcription induces a gradient of protein production transcribing the highest amounts of the 3′ N gene and the lowest amount of the 5′-most L gene. As intracellular N protein concentrations rise, N associates with the genome template, causing a switch from transcription to replication by inducing the production of readthrough (+) full-length genome templates (step 2). Positive RNA synthesis serves as template for the production of full-length negative genomes, which, upon synthesis, are tightly bound by the N protein (step 3). Newly synthesized negative-strand genomes, associated with N, bind additional viral proteins in cooperation with numerous cellular proteins, allowing progeny virus to bud from the infected cell (step 4). During the course of infection, IRF-3 physically associates with the N protein of MeV through the interferon association domain (IAD) and its C-terminal negatively charged domain, leading to the C-terminal phosphorylation of IRF-3 by the virus-activated kinase (VAK) (step 5). Phosphorylation of IRF-3 is followed by its release from N, IRF dimerization, nuclear translocation, DNA binding, association with CBP, and transcriptional activation of the IFN-α/β genes (step 6). IAD, IRF association domain; DBD, DNA binding domain; RBD, RNA binding domain; N/P, hydrophobic domain involved in N/P interactions; and [−], negatively charged domain.

N and dsRNA (data not shown), suggesting that P and dsRNA played an indirect role in the localization of the N protein.

N is a basic protein with high affinity for nucleic acids, since it serves to bind the viral genome during infection (6, 16, 31). However, in the absence of a cytoplasmic template, as is the case during transient expression of N, N localizes to the nucleus; in the presence of a cytoplasmic substrate, N becomes anchored in the cytoplasm (20). Interestingly, at higher concentrations, the overexpression of N alone is sufficient to induce the production of nucleocapsid-like structures through the binding of cellular mRNA (14, 50). Taken together, these data suggest that viral replication is required for the virus-activated kinase activation at low MOIs due to the requirement for N protein accumulation to support nucleocapsid formation. At higher MOIs, the amount of nucleocapsid structures introduced to the cell may be adequate for direct IRF-3 activation (Fig. 8). In addition, the ability of N to associate with both the virus-activated kinase and IRF-3 provides further support for this model of nucleocapsid recognition.

Although it is worth noting that in cells that express constitutive levels of N, there appears to be no phosphorylation, as measured by SDS-PAGE (data not shown). Although difficult to explain, this may represent a threshold of N that is required for IRF-3 activation which is not obtained in the stable cells. This concept is supported by the fact that IRF-3 activation, as measured by electrophoretic mobility shift assay, can be detected when IRF-3 is overexpressed or when higher quantities of N are introduced into these cells by transfection (data not shown).

Additional support for this work derives from the studies of Noe et al., who found that the chemokine RANTES was induced by MeV in an MOI-dependent manner in human astrocytoma-derived U373 cells (38). In their study, Noe et al. determined that expression of the N gene alone in a vaccinia virus expression system was adequate for RANTES production. Although their work suggested that N-induced RANTES was not dependent on protein production, as MeV, in the presence of cycloheximide, was still capable of inducing RANTES production, their use of an MOI of 10 probably allowed delivery of sufficient N protein packaged within the virions themselves. In addition to this, Yang et al. recently published that the capsid protein of West Nile virus was also capable of inducing RANTES production (56). We have previously demonstrated that virus-induced RANTES transcriptional activation is mediated through the cooperativity between IRF-3 and NF-κB (15). Thus, nucleocapsid-mediated virus-activated kinase activation and IRF-3 phosphorylation may provide the molecular basis for RANTES activation.

IRF-3 was originally identified in an express sequence-tagged cDNA library as a 50-kDa ISRE binding protein and later described as a dsRNA-activated factor (DRAF1) (1, 55). Treatment with dsRNA showed association of a 300-kDa cellular protein with IRF-3 (55) and nuclear accumulation of the latter (57). For these reasons, dsRNA has remained the viral product believed to be sufficient for IRF-3 activation. Despite those interesting observations, we were unable to detect any IRF-3-inducible C-terminal phosphorylation or degradation following exposure of Jurkat T cells, U937 cells, and 293 cells to dsRNA (M. Servant, B. tenOever, and J. Hiscott, unpublished data). These discrepancies were further strengthened by the observation that dsRNA-binding proteins, such as vaccinia virus E3L (49) and influenza virus NS1 (52), have been shown to block IRF-3 phosphorylation, whereas other dsRNA-binding proteins, such as DRBP97 and Staufen, were without any effect (49).

Another dsRNA-binding protein, PACT, was recently shown to be a positive regulator of IFN-α and -β through the activation of NF-κB, IRF-3, and IRF-7 (21). As with E3L, the dsRNA-binding activity of PACT was shown to be important but not sufficient for this effect. PACT was found to colocalize with N, which suggests that dsRNA may play a structural role in IRF-3 activation. As the overexpression of N alone has been found to induce the formation of nucleocapsid-like structures through association with nonspecific RNA, it is feasible that dsRNA may also form nucleocapsid-like structures by associating with cellular RNA binding proteins, creating, in both cases, a nucleocapsid-like structure capable of activating IRF-3. The ability of the nucleocapsid protein in the activation of IFNs was demonstrated as early as 1980 in the study by Marcus et al., which clearly showed that vesicular stomatitis virus N was required for the induction of interferon-inducing particles (32).

Finally, these experiments demonstrate for the first time that IRF-3 activation represents a novel target in the cellular recognition of virus infection. The ubiquitous IRF-3 protein serves as a direct recognition sensor of the MeV nucleocapsid structure that encapsidates viral RNA. This interaction is believed to be directly responsible for the phosphorylation and activation of IRF-3, leading to the triggering of the IFN-α/β antiviral response.

ACKNOWLEDGMENTS

We thank M. A. Billeter (University of Zurich) for the recombinant MeV constructs and cell lines and Paula Pitha and Brian Ward for reagents used in this study. We also thank members of the Molecular Oncology Group of the Lady Davis Institute for helpful discussions.

This work was supported by grants to J.H. from the Canadian Institutes of Health Research and CANVAC, the Canadian Network for Vaccines and Immunotherapeutics. M.J.S. and J.H. were supported by Postdoctoral Fellowship and Senior Scientist awards, respectively, from CIHR. N.G. was supported with a Postdoctoral Fellowship from Fonds de la Recherche en Santé du Quebec.

REFERENCES

1. **Au, W.-C., P. A. Moore, W. Lowther, Y.-T. Juang, and P. M. Pitha.** 1995. Identification of a member of the interferon regulatory factor family that binds to the interferon-stimulated response element and activates expression of interferon-induced genes. Proc. Natl. Acad. Sci. USA **92:**11657–11661.
2. **Azimi, N., Y. Tagaya, J. Mariner, and T. A. Waldmann.** 2000. Viral activation of interleukin-15 (IL-15): characterization of a virus-inducible element in the IL-15 promoter region. J. Virol. **74:**7338–7348.
3. **Banerjee, A. K.** 1987. Transcription and replication of rhabdoviruses. Microbiol. Rev. **51:**66–87.
4. **Banerjee, A. K., S. Barik, and B. P. De.** 1991. Gene expression of nonsegmented negative strand RNA viruses. Pharmacol. Ther. **51:**47–70.
5. **Blumberg, B. M., M. Leppert, and D. Kolakofsky.** 1981. Interaction of VSV leader RNA and nucleocapsid protein may control VSV genome replication. Cell **23:**837–845.
6. **Buckland, R., P. Giraudon, and F. Wild.** 1989. Expression of MeV nucleoprotein in Escherichia coli: use of deletion mutants to locate the antigenic sites. J. Gen. Virol. **70:**435–441.
7. **Casola, A., N. Burger, T. Liu, M. Jamaluddin, A. R. Brasier, and R. P. Garofalo.** 2001. Oxidant tone regulates RANTES gene expression in airway epithelial cells infected with respiratory syncytial virus. Role in viral-induced interferon regulatory factor activation. J. Biol. Chem. **276:**19715–19722.
8. **Cattaneo, R., G. Rebmann, K. Baczko, V. ter Meulen, and M. A. Billeter.** 1987. Altered ratios of MeV transcripts in diseased human brains. Virology **160:**523–526.

9. **Chu, W.-M., D. Ostertag, Z.-W. Li, L. Chang, Y. Chen, Y. Hu, B. Williams, J. Perrault, and M. Karin.** 1999. JNK2 and IKKβ are required for activating the innate response to viral infection. Immunity **11:**721–731.
10. **Delhase, M., M. Hayakawa, Y. Chen, and M. Karin.** 1999. Positive and negative regulation of the IκB kinase activity through IKKβ subunit phosphorylation. Science **284:**309–313.
11. **Di Stefano, R., G. Burgio, P. Ammatuna, A. Sinatra, and A. Chiarini.** 1976. Thermal and ultraviolet inactivation of plaque purified MeV clones. J. Bacteriol. Virol. Immunol. **69:**3–11.
12. **Du, W., D. Thanos, and T. Maniatis.** 1993. Mechanisms of transcriptional synergism between distinct virus-inducible enhancer elements. Cell **74:**887–898.
13. **Falvo, J. V., B. S. Parekh, C. H. Lin, E. Fraenkel, and T. Maniatis.** 2000. Assembly of a functional beta interferon enhanceosome is dependent on ATF-2–c-Jun heterodimer orientation. Mol. Cell. Biol. **20:**4814–4825.
14. **Fooks, A. R., E. Schadeck, U. G. Liebert, A. B. Dowsett, B. K. Rima, M. Steward, J. R. Stephenson, and G. W. Wilkinson.** 1995. High-level expression of the MeV nucleocapsid protein by using a replication-deficient adenovirus vector: induction of an MHC-1-restricted CTL response and protection in a murine model. Virology **210:**456–465.
15. **Genin, P., M. Algarte, P. Roof, R. Lin, and J. Hiscott.** 2000. Regulation of RANTES chemokine gene expression requires cooperativity between NF-kappa B and IFN-regulatory factor transcription factors. J. Immunol. **164:** 5352–5361.
16. **Gombart, A. F., A. Hirano, and T. C. Wong.** 1993. Conformational maturation of MeV nucleocapsid protein. J. Virol. **67:**4133–4141.
17. **Hamaguchi, M., T. Yoshida, K. Nishikawa, H. Naruse, and Y. Nagai.** 1983. Transcriptive complex of Newcastle disease virus. I. Both L and P proteins are required to constitute an active complex. Virology **128:**105–117.
18. **Heylbroeck, C., S. Balachandran, M. J. Servant, C. DeLuca, G. N. Barber, R. Lin, and J. Hiscott.** 2000. The IRF-3 transcription factor mediates Sendai virus-induced apoptosis. J. Virol. **74:**3781–3792.
19. **Horikami, S. M., and S. A. Moyer.** 1991. Synthesis of leader RNA and editing of the P mRNA during transcription by purified MeV. J. Virol. **65:**5342–5347.
20. **Huber, M., R. Cattaneo, P. Spielhofer, C. Orvell, E. Norrby, M. Messerli, J. C. Perriard, and M. A. Billeter.** 1991. MeV phosphoprotein retains the nucleocapsid protein in the cytoplasm. Virology **185:**299–308.
21. **Iwamura, T., M. Yoneyama, K. Yamaguchi, W. Suhara, W. Mori, K. Shiota, Y. Okabe, H. Namiki, and T. Fujita.** 2001. Induction of IRF-3/-7 kinase and NFκB in response to double-stranded RNA and virus infection: common and unique pathways. Genes Cells **6:**375–388.
22. **Juang, Y. T., W. Lowther, M. Kellum, W. C. Au, R. Lin, J. Hiscott, and P. M. Pitha.** 1998. Primary activation of interferon A and interferon B gene transcription by interferon regulatory factory-3. Proc. Natl. Acad. Sci. USA **95:**9837–9842.
23. **Kim, T. K., and T. Maniatis.** 1998. The mechanism of transcriptional synergy of an in vitro assembled interferon-β enhanceosome. Mol. Cell **1:**119–129.
24. **Kolakofsky, D.** 1982. A model for the control of nonsegmented negative strand viruses genome replication. Virus Persistence Symp. 33. Cambridge University Press, Cambridge, Mass.
25. **Kumar, K. P., K. M. McBride, B. K. Weaver, C. Dingwall, and N. C. Reich.** 2000. Regulated nuclear-cytoplasmic localization of interferon regulatory factor 3, a subunit of double-stranded RNA-activated factor 1. Mol. Cell. Biol. **20:**4159–4168.
26. **Leblanc, J.-F., L. Cohen, M. Rodrigues, and J. Hiscott.** 1990. Synergism between distinct enhanson domains in viral induction of the human beta interferon gene. Mol. Cell. Biol. **10:**3987–3993.
27. **Lin, R., C. Heylbroeck, P. Genin, P. Pitha, and J. Hiscott.** 1999. Essential role of IRF-3 in direct activation of RANTES gene transcription. Mol. Cell. Biol. **19:**959–966.
28. **Lin, R., C. Heylbroeck, P. M. Pitha, and J. Hiscott.** 1998. Virus-dependent phosphorylation of the IRF-3 transcription factor regulates nuclear translocation, transactivation potential, and proteasome-mediated degradation. Mol. Cell. Biol. **18:**2986–2996.
29. **Lin, R., Y. Mamane, and J. Hiscott.** 1999. Structural and functional analysis of interferon regulatory factor 3: localization of the transactivation and autoinhibitory domains. Mol. Cell. Biol. **19:**2465–2474.
30. **Lin, R., P. Genin, Y. Mamane, and J. Hiscott.** 2000. Selective DNA binding and association with CBP coactivator contribute to differential activation of type 1 interferon genes by interferon regulatory factors 3 and 7. Mol. Cell. Biol. **20:**6342–6353.
31. **Liston, P., R. Batal, C. DiFlumeri, and D. J. Briedis.** 1997. Protein interaction domains of the MeV nucleocapsid protein (NP). Arch. Virol. **142:**305–321.
32. **Marcus, P. I., and M. J. Sekellick.** 1980. Interferon induction by viruses. III. Vesicular stomatitis virus: interferon-inducing particle activity requires partial transcription of gene N. J. Gen. Virol. **47:**89–96.
33. **Marie, J. C., J. Kehren, M. C. Trescol-Biemont, A. Evlashev, H. Valentin, T. Walzer, R. Tedone, B. Loveland, J. F. Nicolas, C. Rabourdin-Combe, and B. Horvat.** 2001. Mechanism of MeV-induced suppression of inflammatory immune responses. Immunity **14:**69–79.
34. **Matsuyama, T., T. Kimura, M. Kitagawa, N. Watanabe, T. Kundig, R. Amakawa, K. Kishihara, A. Wakeham, J. Potter, C. Furlonger, A. Narendran, H. Suzuki, P. Ohashi, C. Paige, T. Taniguchi, and T. Mak.** 1993. Targeted disruption of IRF-1 or IRF-2 results in abnormal type I IFN induction and aberrant lymphocyte development. Cell **75:**83–97.
35. **Merika, M., A. J. Williams, G. Chen, T. Collins, and D. Thanos.** 1998. Recruitment of CBP/p300 by the IFNβ enhanceosome is required for synergistic activation of transcription. Mol. Cell **1:**277–287.
36. **Miyamoto, M., T. Fujita, Y. Kimura, M. Maruyama, H. Harada, Y. Sudo, T. Miyata, and T. Taniguchi.** 1988. Regulated expression of a gene encoding a nuclear factor, IRF-1, that specifically binds to the IFN-β gene regulatory elements. Cell **54:**903–913.
37. **Navarro, L., K. Mowen, S. Rodems, B. Weaver, N. Reich, D. Spector, and M. David.** 1998. Cytomegalovirus activates interferon immediate-early response gene expression and an interferon regulatory factor 3-containing interferon-stimulated response element-binding complex. Mol. Cell. Biol. **18:**3796–3802.
38. **Noe, K. H., C. Cenciarelli, S. A. Moyer, P. A. Rota, and M. L. Shin.** 1999. Requirements for MeV induction of RANTES chemokine in human astrocytoma-derived U373 cells. J. Virol. **73:**3117–3124.
39. **Preston, C. M., A. N. Harman, and M. J. Nicholl.** 2001. Activation of interferon response factor-3 in human cells infected with herpes simplex virus type 1 or human cytomegalovirus. J. Virol. **75:**8909–8916.
40. **Radecke, F., P. Spielhofer, H. Schneider, K. Kaelin, M. Huber, C. Dotsch, G. Christiansen, and M. A. Billeter.** 1995. Rescue of MeVes from cloned DNA. EMBO J. **14:**5773–5784.
41. **Reis, L. F. L., H. Ruffner, G. Stark, M. Aguet, and C. Weissmann.** 1994. Mice devoid of interferon regulatory factor 1 (IRF-1) show normal expression of type I interferon genes. EMBO J. **13:**4798–4806.
42. **Ronco, L., A. Karpova, M. Vidal, and P. Howley.** 1998. Human papillomavirus 16 E6 oncoprotein binds to interferon regulatory factor-3 and inhibits its transcriptional activity. Genes Dev. **12:**2061–2072.
43. **Samuel, C. E.** 2001. Antiviral actions of interferons. Clin. Microbiol. Rev. **14:**778–809.
44. **Sato, M., H. Suemori, N. Hata, M. Asagiri, K. Ogasawara, K. Nakao, T. Nakaya, M. Katsuki, S. Noguchi, N. Tanaka, and T. Taniguchi.** 2000. Distinct and essential roles of transcription factors IRF-3 and IRF-7 in response to viruses for IFN-alpha/beta gene induction. Immunity **13:**539–548.
45. **Sato, M., N. Tanaka, N. Hata, E. Oda, and T. Taniguchi.** 1998. Involvement of IRF family transcription factor IRF-3 in virus-induced activation of IFN-β gene. FEBS Lett. **425:**112–116.
46. **Schafer, S. L., R. Lin, P. A. Moore, J. Hiscott, and P. M. Pitha.** 1998. Regulation of type 1 interferon gene expression by interferon regulatory factor 3. J. Biol. Chem. **273:**2714–2720.
47. **Schmid, A., R. Cattaneo, and M. A. Billeter.** 1987. A procedure for selective full-length cDNA cloning of specific RNA species. Nucleic Acids Res. **15:** 3987–3996.
48. **Servant, M. J., B. tenOever, C. LePage, L. Conti, S. Gessani, I. Julkunen, R. Lin, and J. Hiscott.** 2001. Identification of distinct signaling pathways leading to the phosphorylation of interferon regulatory factor 3. J. Biol. Chem. **276:**355–363.
49. **Smith, E. J., I. Marie, A. Prakash, A. Garcia-Sastre, and D. E. Levy.** 2001. IRF3 and IRF7 phosphorylation in virus-infected cells does not require double-stranded RNA-dependent protein kinase R or IκB kinase but is blocked by vaccinia virus E3L protein. J. Biol. Chem. **276:**8951–8957.
50. **Spehner, D., R. Drillien, and P. M. Howley.** 1997. The assembly of the MeV nucleoprotein into nucleocapsid-like particles is modulated by the phosphoprotein. Virology **232:**260–268.
51. **Sundstrom, J. B., L. K. McMullan, C. F. Spiropoulou, W. C. Hooper, A. A. Ansari, C. J. Peters, and P. E. Rollin.** 2001. Hantavirus infection induces the expression of RANTES and IP-10 without causing increased permeability in human lung microvascular endothelial cells. J. Virol. **75:**6070–6085.
52. **Talon, J., C. M. Horvath, R. Polley, C. F. Basler, T. Muster, P. Palese, and A. Garcia-Sastre.** 2000. Activation of interferon regulatory factor 3 is inhibited by the influenza A virus NS1 protein. J. Virol. **74:**7989–7996.
53. **Thanos, D., and T. Maniatis.** 1995. Virus induction of human IFNβ gene expression requires the assembly of an enhanceosome. Cell **83:**1091–1100.
54. **Wathelet, M. G., C. H. Lin, B. S. Parakh, L. V. Ronco, P. M. Howley, and T. Maniatis.** 1998. Virus infection induces the assembly of coordinately activated transcription factors on the IFN-β enhancer in vivo. Mol. Cell **1:**507–518.
55. **Weaver, B. K., K. P. Kumar, and N. C. Reich.** 1998. Interferon regulatory factor 3 and CREB-binding protein/p300 are subunits of double-stranded RNA-activated transcription factor DRAF1. Mol. Cell. Biol. **18:**1359–1368.
56. **Yang, J. S., J. J. Kim, D. Hwang, A. Y. Choo, K. Dang, H. Maguire, S. Kudchodkar, M. P. Ramanathan, and D. B. Weiner.** 2001. Induction of potent Th1-type immune responses from a novel DNA vaccine for West Nile virus New York isolate (WNV-NY1999). J. Infect. Dis. **184:**809–816.
57. **Yoneyama, M., W. Suhara, Y. Fukuhara, M. Fukada, E. Nishida, and T. Fujita.** 1998. Direct triggering of the type I interferon system by virus infection: activation of a transcription factor complex containing IRF-3 and CBP/p300. EMBO J. **17:**1087–1095.